Neurochemical Research (2019) 44:2460–2469
https://doi.org/10.1007/s11064-019-02882-6

BRIEF COMMUNICATION

Protective Effects of ACY-1215 Against Chemotherapy-Related Cognitive Impairment and Brain Damage in Mice

Dongmei Wang[1] · Bei Wang[1] · Yumei Liu[2] · Xiaohui Dong[1] · Yanwei Su[1] · Sanqiang Li[1]

Received: 13 June 2019 / Revised: 29 August 2019 / Accepted: 18 September 2019 / Published online: 30 September 2019

Abstract

Chemotherapy-related cognitive impairment (CRCI) is a potential long-term side effect during cancer treatment. There are currently no effective treatments for CRCI. Reduction or inhibition of histone deacetylase 6 (HDAC6) has been considered a possible therapeutic strategy for cognitive deficits. HDAC6 inhibition recently has been shown to reverse chemotherapy-induced peripheral neuropathy effectively. In the present study, we examined the effect of HDAC6 inhibitor ACY-1215 (Ricolinostat) on cisplatin-induced brain damage and cognitive deficits in mice. Our results showed that ACY-1215 ameliorated behavioral deficits and dendritic spine loss and increased synaptic density in cisplatin-treated mice. Mechanistically, HDAC6 inhibitor ACY-1215 enhanced α-tubulin acetylation in the hippocampus of cisplatin-treated mice. Furthermore, ACY-1215 recovered cisplatin-induced impaired mitochondrial transport and mitochondrial dysfunction in the hippocampus. Our results suggest that inhibition of HDAC6 improves established cisplatin-induced cognitive deficits by the restoration of mitochondrial and synaptic impairments. These results offer prospective approaches for CRCI, especially because ACY1215 currently serves as an add-on cancer therapy during clinical trials.

Graphic Abstract

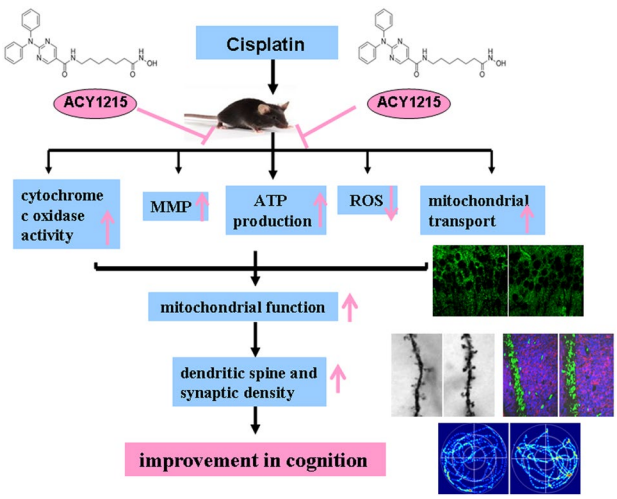

Keywords HDAC6 · Chemotherapy · Cognitive · Cisplatin

Abbreviations

CRCI	Chemotherapy-related cognitive impairment
HDAC6	Histone deacetylase 6
MMP	Mitochondrial membrane potential
mtDNA	Mitochondria DNA
MWM	Morris water maze

Electronic supplementary material The online version of this article (https://doi.org/10.1007/s11064-019-02882-6) contains supplementary material, which is available to authorized users.

Extended author information available on the last page of the article

nDNA	Nuclear DNA
NOR	Novel object recognition
ROS	Reactive oxygen species
PSD95	Postsynaptic density protein 95
vGlut1	Vesicular glutamate transporter type 1

Introduction

Development in the efficacy of cancer treatment has led to a significant increase in survival rate and an obviously reduced risk of recurrence [1]. However, many survivors suffer from the long-term severe neurotoxic side effects of cancer therapy. One consequence of modern cancer treatment is chemotherapy-related cognitive impairment (CRCI), commonly known as "chemobrain". CRCI exhibits a broad range of neurological problems, clinically manifested by decrements in executive functioning, memory, attention, and processing speed [2, 3]. CRCI has become an increasing problem of significant clinical concern, up to 34% of patients experiencing persistent cognitive problems years after cessation of chemotherapy [4].

Platinum-based chemotherapeutic agents, such as cisplatin, are part of standard treatment for numerous malignancies, including head, ovarian, bladder, lung, and testis cancer. Cisplatin treatment is correlated with a high incidence of CRCI, and it causes mechanical allodynia, numbness, and spontaneous pain in the rodent. Cisplatin can cross the blood-brain barrier, penetrate the brains, and accumulate in the hippocampus [5, 6]. Cisplatin, a DNA targeting agent, binds to the guanine residues in DNA and forms toxic platinum DNA adducts to induce DNA damage and apoptosis [7]. Unlike nuclear DNA (nDNA), mitochondrial DNA (mtDNA) is more susceptible than nDNA to damage from cisplatin and has been proposed as a particular target for cisplatin genotoxicity [8, 9]. Cisplatin forms adducts with mtDNA, inhibits mtDNA replication and mitochondrial gene transcription, and impairs mitochondrial function. The mitochondrial dysfunction in the brains is considered to play a vital role in CRCI [10, 11]. Cisplatin has been shown to induce mitochondrial DNA damage and cause mitochondrial swelling or vacuolization in primary cultured hippocampal neurons [10]. In the brains of cisplatin-treated mice, these mitochondrial morphological changes are associated with decreased respiratory capacity and impaired mitochondrial function. Furthermore, that prevention of cisplatin-evoked mitochondrial abnormalities by the compound pifithrin-μ also rescued cisplatin-elicited cognitive impairment [12]. This evidence further supports a causal link between mitochondrial damage and CRCI.

Histone deacetylase 6 (HDAC6), a member of the class IIB HDACs, deacetylates many non-histone proteins such as α-tubulin, peroxiredoxin, and HSP90. HDAC6 is a promising target for treating neurodegenerative diseases. Importantly, HDAC6 is involved in the modulation of mitochondrial transport [13, 14]. Pharmacological inhibition of HDAC6 can increase α-tubulin acetylation and promote mitochondrial transport in primary cultured hippocampal neurons [15]. HDAC6 inhibitor ACY-1215 improved microtubule stability via increasing α-tubulin acetylation and alleviated behavioral impairment in a mouse model of Alzheimer's disease [16]. Recently, ACY-1215 was reported to reverse cisplatin-evoked peripheral neuropathy by the restoration of mitochondrial function in dorsal root ganglia [17]. Besides, ACY1215 currently serves as an add-on cancer therapy during clinical trials (https://clinicaltrials.gov/ct2/show/NCT02632071?term=ricolinostat&rank=3, and https://clinicaltrials.gov/ct2/show/NCT02661815?term=ricolinostat&rank=6). However, little is known about the effects of ACY-1215 on the CRCI. Therefore, the purpose of the present study is to investigate the impact of ACY-1215 on cisplatin-induced cognitive deficits in mice and to identify potential mechanisms related to the protective effects of HDAC6 inhibition.

Materials and Methods

Group and Treatment

C57BL/6 male mice were randomly assigned into four groups (n = 14): control group, ACY-1215 group, Cisplatin group, and Cisplatin/ACY-1215 group. Mice were intraperitoneally (i.p.) administered with cisplatin (2.3 mg/kg per day, Sigma-Aldrich) or saline for three cycles consisting of 5 daily injections followed by a 5-day rest with no injection. The total cumulative dose of cisplatin was 34.5 mg/kg [18]. ACY-1215 (50 mg/kg, Selleck) or vehicle (5% dimethyl sulfoxide in saline) was treated intraperitoneally starting 1 h prior to each cisplatin injection for consecutive 30 days. The doses of ACY-1215 were selected based on other experimental studies [16, 19]. The experimental animal protocol was approved by the Institutional Animal Experiment Committee of Henan University of Science and Technology, China.

Novel Object Recognition and Morris Water Maze

The novel object recognition (NOR) and the Morris water maze (MWM) tests were employed to evaluate the cognitive function of the mice. The NOR test was conducted as previously described with minor modifications [20]. Briefly, each mouse was placed into a testing arena (40 cm × 40 cm × 40 cm) with two identical objects and allowed to explore for 5 min during the training phase. In the test phase, each mouse was transferred back to the arena with a familiar object and a novel object. The exploration time for the familiar (TF) or

the novel object (TN) during the test phase was recorded. The discrimination index was determined by the equation (TN − TF) / (TN + TF).

The MWM test consists of a circular tank (100 cm in diameter) and a platform (10 cm in diameter). The circular pool filled with warm water (22 ± 1 °C) was divided into four equal quadrants, and the platform (10 cm in diameter) was placed 1 cm below the surface of the water at the midpoint of one quadrant. The swimming behavior of all mice was monitored and analyzed by EthoVision video tracking system (Version XT Noldus. Wageningen, Netherlands). During the memory acquisition phase, each mouse was subjected to four training trials for five consecutive days. The escape latency (the time to find the platform) was recorded, and the average of four trials was determined. Memory retention was evaluated on the 6th day, and each mouse was allowed to swim freely for 60 s without the platform. The parameters measured included the time spent in the target quadrant and the velocity during the probe test.

Pharmacokinetics Profiling

For PK analysis, ACY-1215 was isolated from plasma and brain by protein precipitation using 50:50 (vol/vol) acetonitrile: methanol and analyzed using a high-performance liquid chromatography/mass spectrometry (HPLC/MS/MS) method [19]. The lower limit of quantification for ACY-1215 was 1 ng/mL, and the upper limit was extendable up to 1000 ng/mL.

Mitochondrial Function Analysis

Mitochondrial Isolation

Mice brain mitochondria were isolated as previously described [21, 22]. Briefly, brains were homogenized in isolation buffer (75 mM sucrose, 215 mM mannitol, 1 mM EGTA, 0.1% BSA, 20 mM HEPES (Na^+), pH 7.2). Following low-speed spin, the supernatant was collected and centrifuged at 7000×*g* for 10 min at 4 °C. The mitochondrial pellets were obtained, resuspended in isolation buffer, and centrifuged at 7000×*g* for 10 min at 4 °C. The pellets were resuspended in 14% percoll solution and centrifuged at 13,000×*g* for 10 min at 4 °C. The final mitochondrial pellet was resuspended in resuspension buffer, and the mitochondrial protein concentrations were determined using the BCA Protein Assay Kit (Beyotime, Shanghai, China).

Cytochrome c Oxidase Activity

Cytochrome c oxidase activity was examined as previously described [23]. The isolated mitochondria were mixed with 0.3 mM reduced cytochrome c in 75 mM phosphate buffer, and then the change in absorbance at 550 nm was recorded. Cytochrome c oxidase activity was calculated as [(OD1 − OD2) / (t1 − t2)] / (ε × mg protein) and expressed as nmol of cytochrome c oxidized/min/mg protein.

Mitochondrial ATP Production

Mitochondrial ATP production was assayed using an ATP bioluminescent assay kit (Promega, USA). Mitochondria were promptly incubated with ATP synthesizing substrates for 5 min at 30 °C and then mixed with luciferase enzyme and luciferin substrate. The bioluminescence intensity was assessed using a PerkinElmer microplate reader. The relative light units (RLU) were converted into nmol ATP per mg mitochondrial protein as described in the manual of the kit.

Reactive Oxygen Species (ROS) Production

Mitochondrial ROS production was measured based on the oxidation of 2′,7′-dichlorofluorescein diacetate (DCFH-DA) to fluorescent 2′,7′-dichlorofluorescein (DCF). Briefly, 100 µg isolated mitochondria were incubated with 120 µL of respiration buffer (125 mM KCl, 2.5 mM malate, 5 mM pyruvate, 1 mM $MgCl_2$, 500 µM EGTA, 2 mM KH_2PO_4, 20 mM HEPES, pH 7.0) and DCFH-DA for 20 min. The DCF fluorescence with excitation at 485 nm and emission at 528 nm was read using a PerkinElmer microplate reader.

Mitochondrial Membrane Potential (MMP)

To evaluate MMP, the isolated mitochondria were incubated with 1 mM JC-1 in mitochondrial isolation buffer with 5 mM malate and 5 mM pyruvate. This mixture interacted in a dark room for 20 min, and the fluorescence with excitation at 530 nm and emission at 590 nm was then measured.

Golgi Staining and Analysis of Dendritic Spine Density

Fresh brains were processed for Golgi staining using the FD Rapid GolgiStain kit (FD NeuroTechnologies) following the manufacturer's instructions. Brains were coronally sliced with a thickness of 150 µm using a vibratome (World Precision Instruments) and stained. Images were acquired by using an upright microscope (Leica, Wetzlar, Germany) and processed quantitatively using Image-ProPlus version 6.0. The apical spines on tertiary dendrites of CA1 pyramidal neurons were counted. Spine density was calculated as the number of spines per 10 µm dendrite. Three mice per group were used, and 5–6 random neurons from each sample per mice were analyzed.

Immunofluorescence Staining

Following transcardial perfusion with ice-cold normal saline and 4% paraformaldehyde, the brains were postfixed in 4% paraformaldehyde and switched to 30% sucrose phosphate buffer. Serial 20 μm-thick coronal sections were prepared. Following blocked in 10% goat serum, brain slides were incubated with mouse anti-Neuron (1:500, Millipore, Temecula, USA), rabbit anti-PSD95 (1:300, Cell Signaling Technology, Danvers, MA), and guinea pig anti-vGlut1 (1:500, Synaptic System, Goettingen, Germany) at 4 °C overnight. After rinsed with PBS, the slides were incubated with Alexa 488 conjugated goat anti-mouse IgG (1:500, Invitrogen, Carlsbad, USA), Alexa 594 conjugated goat anti-rabbit IgG (1:500, Invitrogen, Carlsbad, USA), and Alexa 647 conjugated goat anti-guinea pig IgG (1:500, Invitrogen, Carlsbad, USA) at room temperature for 60 min. Images were acquired under a Nikon confocal microscope, and the staining intensity was quantified using Image J software. The synapses were determined by co-localization of vGlut1 and PSD95 followed by three-dimensional reconstruction.

Western Blot Analysis

Protein preparation and immunoblotting procedures were carried out as previously described [24, 25]. The hippocampus was carefully dissected and homogenized in RIPA buffer supplemented with 0.1% protease inhibitor cocktail and 0.1% PMSF. After centrifugation at 14,000×*g* for 30 min at 4 °C, the supernatant was collected, and the BCA Protein Assay Kit (Beyotime, Shanghai, China) was used to determine the protein concentration. Equal amounts of hippocampus soluble protein were separated via SDS-PAGE gel and transferred to a nitrocellulose membrane. Membranes were incubated with anti-acetylated α-tubulin antibody (1:1000, Cell Signaling Technology, Danvers, MA) and anti-α-tubulin antibody (1:1000, Cell Signaling Technology, Danvers, MA) at 4 °C overnight. Following rinsed with TBST, the membranes were incubated for 1 h at room temperature with HRP-conjugated secondary antibodies (Proteintech, Chicago, USA). The immunoreactive proteins on the membrane were visualized using an enhanced chemiluminescent detection system (Thermo, Rockford, CA, USA). Images were acquired by Bio-Rad Chemidoc Imaging System, and the intensity of protein bands was analyzed using Image-Pro Plus software.

Statistical Analysis

Statistical analysis of the experimental data was performed using SPSS (version 11.0). The data were analyzed using one-way ANOVA with Bonferroni post-hoc test. For the Morris water maze test, the differences in the escape latency among the groups were analyzed using two-way analysis of variance (ANOVA) with repeated measures. The criterion for statistical significance was considered at $p < 0.05$.

Results

HDAC6 Inhibitor ACY-1215 Improves Cognitive Impairment in Cisplatin-Treated Mice

The Morris water maze test was employed to examine the effects of HDAC6 inhibitor ACY-1215 on spatial learning and memory impairment induced by cisplatin. In the hidden platform (Fig. 1a), the escape latency in all groups improved over time. Cisplatin-treated mice exhibited a longer time to find the platform compared to the control group, whereas co-administration with ACY-1215 markedly reduced the escape latency. In the subsequent probe test, Cisplatin-treated mice spent less time in the target quadrant than the control group. ACY-1215 plus cisplatin treatment prolonged the duration spent in the target quadrant (Fig. 1b). These results revealed that the impaired spatial learning and memory task induced by cisplatin was rescued by ACY-1215. Besides, we test the recognition memory by the NOR test. The discrimination index, decreased in the cisplatin-treated mice, was improved in ACY-1215 plus cisplatin mice (Fig. 1d). ACY-1215 treatment did not prevent cisplatin-induced loss of body weight (Fig. S1). Collectively, these data suggest that HDAC6 inhibitor ACY-1215 can prevent cisplatin-induced cognitive impairment.

Furthermore, ACY-1215 levels were measured in brain and plasma samples using HPLC. Untreated mice demonstrated that ACY-1215 levels were below quantifiable limits for both brain and plasma samples. The mean brain level of ACY-1215 at 0.25, 1, and 4 h after the last dose was 71.37 ng/g, 46.35 ng/g, and 23.32 ng/g, respectively, in Cisplatin/ACY-1215 group and 79.34 ng/g, 48.23 ng/g, and 26.11 ng/g, respectively, in ACY-1215 group. The plasma concentration of ACY-1215 at 0.25, 1, and 4 h after the last dose was 1621.21 ng/mL, 890.32 ng/mL, and 684.67 ng/mL, respectively, in Cisplatin/ACY-1215 group and 1689.11 ng/mL, 1090.48 ng/mL, and 686.81 ng/mL, respectively, in ACY-1215 group (Fig. 2).

HDAC6 Inhibitor ACY-1215 Ameliorates Mitochondrial Dysfunction and Mitochondrial Transport Deficits in Cisplatin-Treated Mice

Cisplatin induced mitochondrial damage as evidenced by a 42.9% decrease in cytochrome c oxidase activity ($p < 0.01$), a 44.7% decrease in ATP production ($p < 0.01$), a 96.4% increase in ROS production ($p < 0.01$), and a 28.6% decrease in MMP ($p < 0.05$) in the brains as compared to controls,

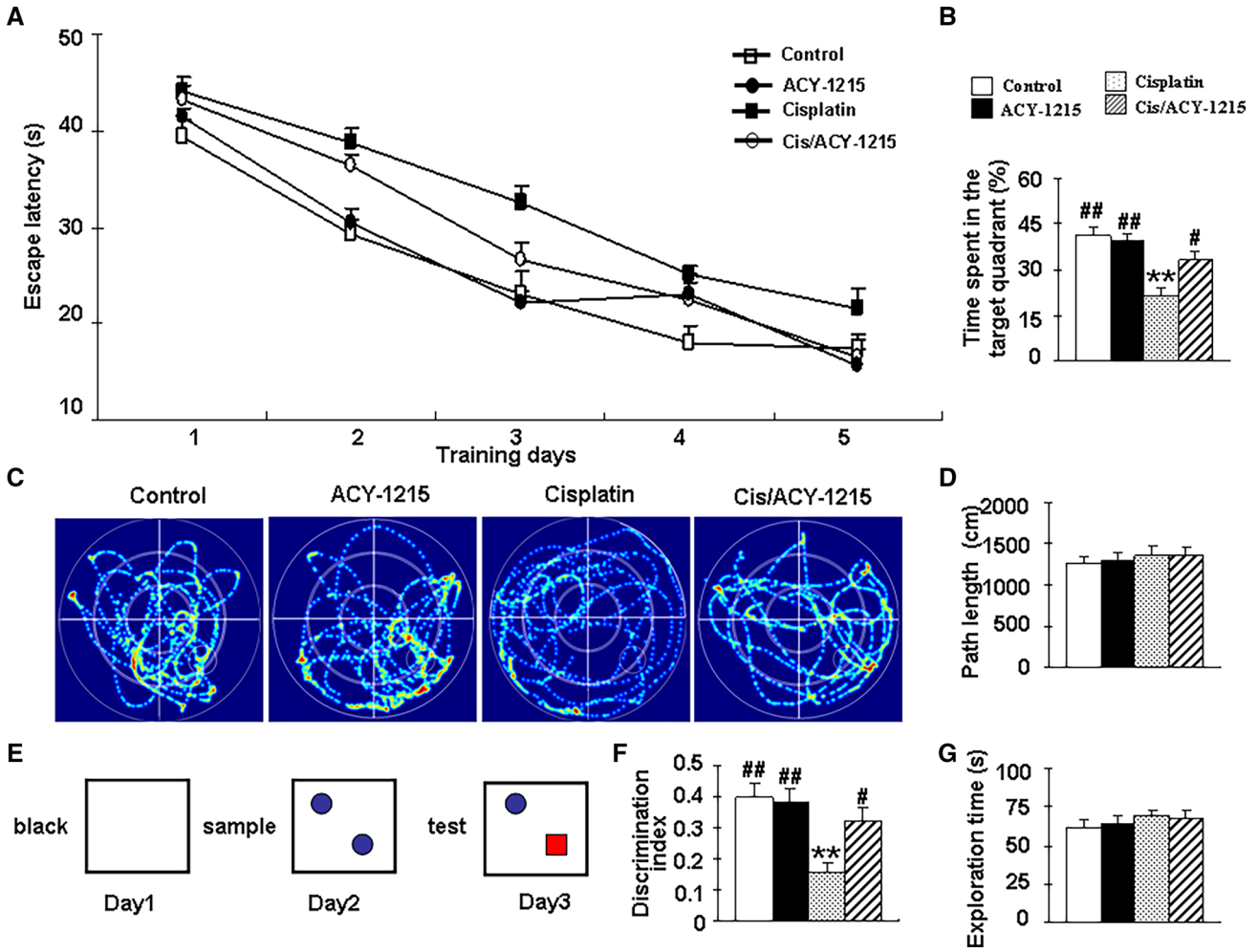

Fig. 1 HDAC6 inhibitor ACY-1215 improves cisplatin-induced cognitive impairment in mice. Mice were administered three cycles of cisplatin treatment (5 daily injections of 2.3 mg/kg followed by a 5-day rest) with or without ACY-1215 (50 mg/kg i.p.). **a** Escape latency during 5 days of hidden platform tests. **b** The percentage of time spent in the target quadrant in the probe test. **c** Movement tracks in the probe test. **d** The path length in the probe test. **e** Set up for the novel object recognition task. **f** The recognition index in the test section of the novel object recognition task. **g** The total interaction time with novel and familiar object in the novel object recognition task. All data are presented as mean ± SEM (n = 12–14, * $p < 0.05$, ** $p < 0.01$ versus control mice; $^{\#}p < 0.05$, $^{\#\#}p < 0.01$ versus cisplatin-treated mice)

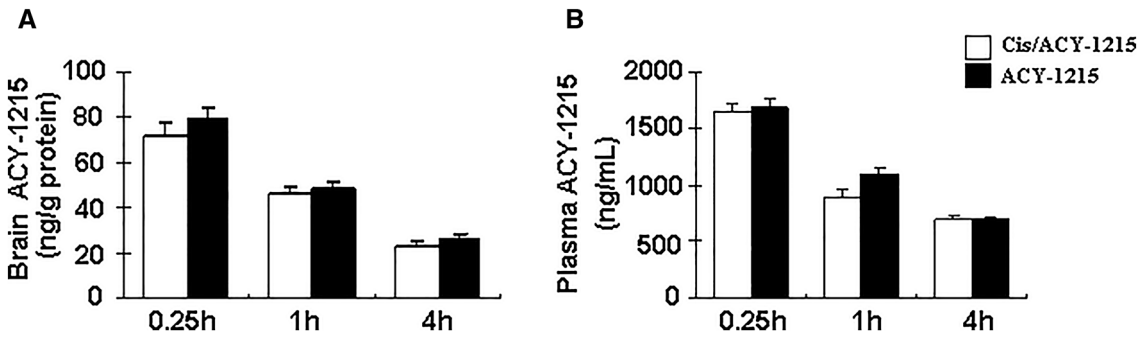

Fig. 2 Pharmacokinetic profile of HDAC6 inhibitor ACY-1215. **a** The mean brain level of ACY-1215 from mice received ACY-1215 (50 mg/kg) with or without cisplatin treatment at 0.25, 1, and 4 h after the last dose. **b** The mean plasma level of ACY-1215 from mice received ACY-1215 (50 mg/kg) with or without cisplatin treatment at 0.25, 1, and 4 h after the last dose

whereas co-administration with ACY-1215 significantly attenuated cisplatin-induced brain mitochondrial dysfunction as indicated by increasing cytochrome c oxidase activity (Fig. 3a), increasing ATP production (Fig. 3b), reducing ROS production (Fig. 3c), and rising MMP (Fig. 3d) by 51.3%, 33.3%, 36.4%, and 22.3%, respectively. In addition, immunoreactivity to Tom20, a marker for mitochondrial localization, was analyzed in mouse brains as previously described [26, 27]. Our results revealed a striking increase in the ratio of Tom20 immunoreactivity in the soma to that in the stratum radiatum in cisplatin-treated mice compared to controls, suggesting impaired mitochondrial transport and subsequent somatic mitochondrial accumulation in cisplatin-treated mice. However, this ratio in cisplatin/ACY-1215 mice was markedly lower than cisplatin-treated mice (Fig. 3e). Elevated acetylation of α-tubulin by HDAC6 inhibition is related to improved mitochondrial transport. Next, the levels of α-tubulin acetylation in the hippocampus of mice were examined by western blotting. We found an apparent reduction in the level of acetylated α-tubulin in the hippocampus of the cisplatin-treated mice compared to controls, which was reversed by ACY-1215 (Fig. 3f).

HDAC6 Inhibitor ACY-1215 Rescues Dendritic Spine and Synaptic Density in the CA1 Region of the Hippocampus in Cisplatin-Treated Mice

Cisplatin-induced mitochondrial damage has been shown to contribute to dendritic spine loss and synaptic injury [10, 18]. Golgi-stained was used to determine the effects of ACY-1215 on the dendritic spine in cisplatin-treated mice. Consistent with previous studies [18], a significant decrease in dendritic spine density was observed in cisplatin-treated mice compared with controls. This defect in spine density was partially rescued by HDAC6 inhibitor ACY-1215 treatment (Fig. 4a). The pronounced change in dendritic spine density led us to evaluate the effects of ACY-1215 on synaptic density. The cisplatin-treated mice exhibited a significant reduction in synaptic density measured by co-localization of vGlut1 and PSD95 compared with controls. This decrease

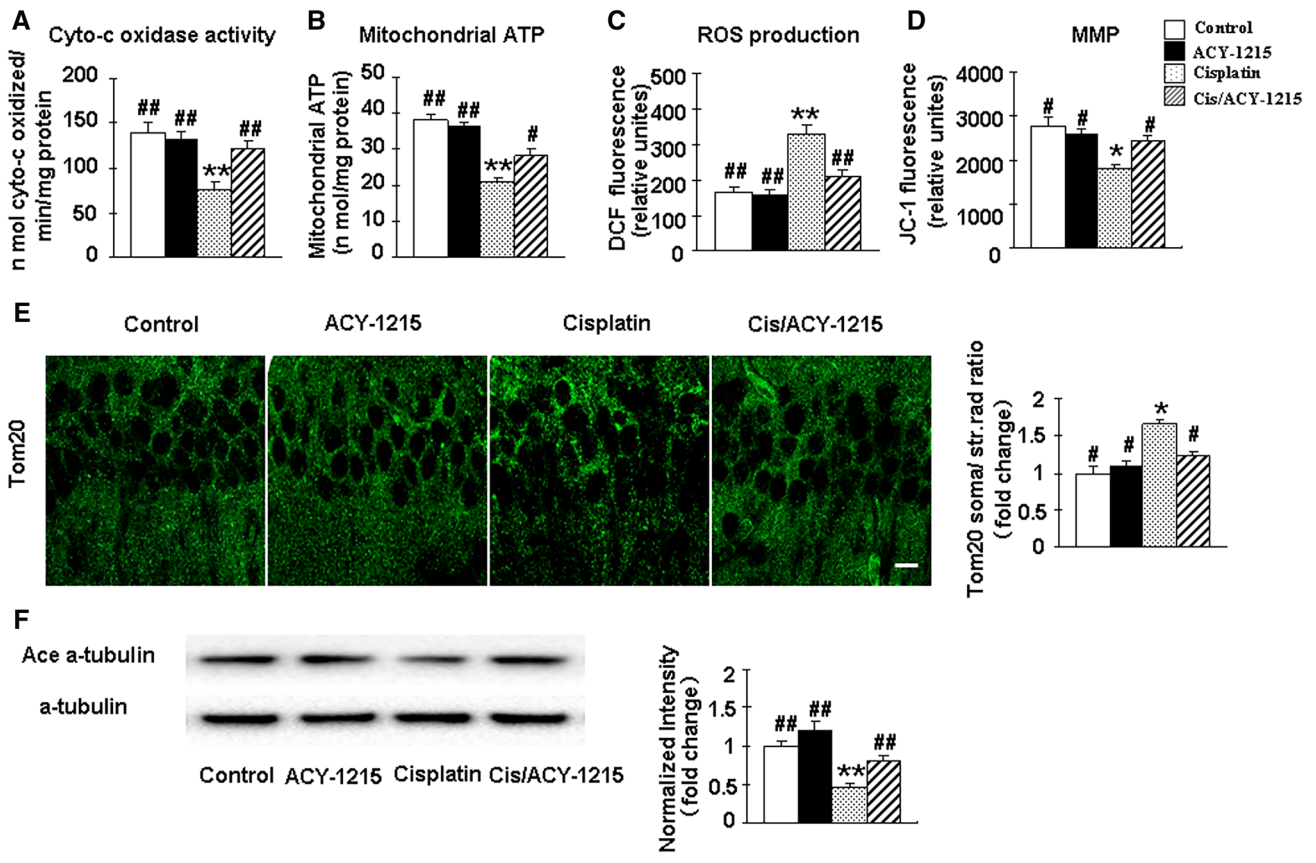

Fig. 3 HDAC6 inhibitor ACY-1215 attenuates mitochondrial dysfunction and rescues mitochondrial transport in cisplatin-treated mice. Brain mitochondria were separated and collected. **a** Cytochrome c oxidase activity. **b** Mitochondrial ATP levels. **c** ROS production. **d** MMP. **e** Left panel: representative confocal images of Tom20 immunoreactivity in the hippocampus of mice (scale bars 10 μm). Right panel: quantification of Tom20 immunoreactivity. **f** Western blot of α-tubulin acetylation in the hippocampus. All data are presented as mean ± SEM (n = 3–4 per group, * $p < 0.05$, ** $p < 0.01$ versus control mice; $^{\#}p < 0.05$, $^{\#\#}p < 0.01$ versus cisplatin-treated mice)

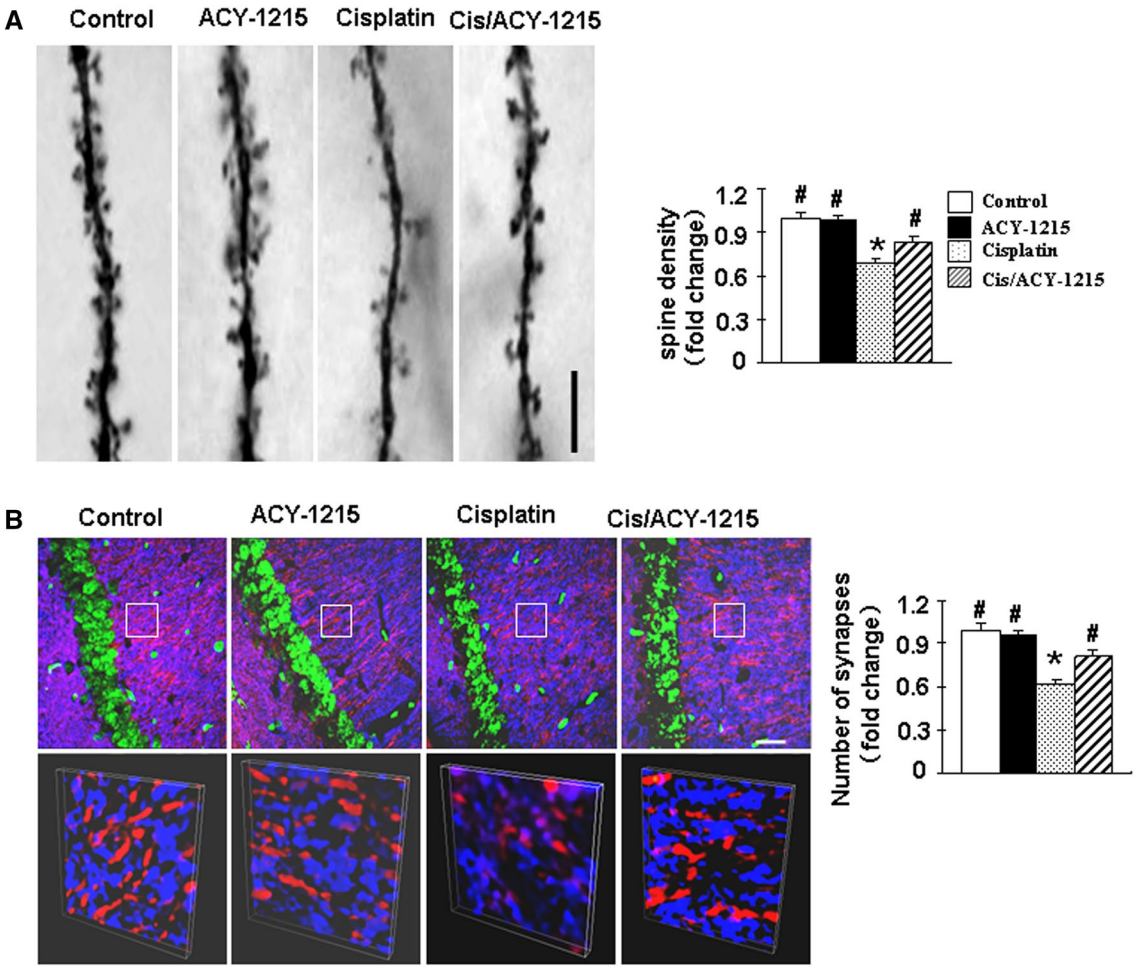

Fig. 4 HDAC6 inhibitor ACY-1215 prevents dendritic spine loss and synaptic injury in the CA1 region of the hippocampus in cisplatin-treated mice. **a** Left panel: representative images of dendritic spines of CA1 apical tertiary dendrites from Golgi-Cox staining (scale bars 10 μm). Right panel: the quantitative analysis of spine density. **b** Upper left panel: representative confocal images visualized with anti-vGLUT1 (blue), anti-PSD95 (red), and anti-NeuN (green) (scale bars, 50 μm); lower left panel: the synapses determined by co-localization of vGlut1 and PSD95 followed by three-dimensional reconstruction. Right panel: the quantitative analysis of synapses. All data are presented as mean ± SEM (n = 3–4 per group, * $p < 0.05$ versus control mice; $^{\#}p < 0.05$ versus cisplatin-treated mice) (Color figure online)

in synaptic density in cisplatin-treated mice was partially rescued by HDAC6 inhibitor ACY-1215 treatment (Fig. 4b).

Discussion

In this present study, pharmacological inhibition of HDAC6 with ACY1215 ameliorated cisplatin-induced cognitive impairment. ACY1215 administration attenuated cisplatin-induced dendritic spine loss and reduction in synaptic density. The reversal of cisplatin-induced cognitive impairment and synaptic damage by HDAC6 inhibition was correlated with restoration of mitochondrial axonal transport deficits and mitochondrial dysfunction in the hippocampus.

Increasing evidence indicates that neural mitochondrial damage may be a central mechanism for chemotherapy-related cognitive impairments [10, 12] and neurotoxicity [28, 29]. MtDNA is more susceptible to damage from cisplatin than nDNA due to limited DNA repair capacity [30, 31]. It has been demonstrated that the levels of cisplatin-mtDNA adducts are much higher than that of cisplatin-nDNA adducts. The preferential formation of mtDNA adducts attributes to a higher degree of initial binding and lack of removal [32]. Cisplatin-induced mitochondrial dysfunction has also been observed in the liver [33], nephrons [34], cultured neurons [31], and brains [35]. Pathological changes in mitochondria are characterized alterations in the mitochondrial respiratory functions, mitochondrial energy failure, impaired mitochondrial axonal transport, and oxidative stress. Consistent with this, the results of the current study also demonstrated brain mitochondrial damage, as evidenced by the decreased cytochrome c oxidase activity, the

ATP deficiency, the increased ROS and the mitochondrial axonal transport deficits in cisplatin-treated mice. Inhibition of HDAC6 has been proposed to exert neuroprotection against neurological disorders by facilitating mitochondrial transport throughout the neuronal network [36–38]. HDAC6 is a well-known α-tubulin deacetylase, and inhibition of HDAC6 increases α-tubulin acetylation [13]. Acetylation of α-tubulin can enhance microtubule stability, recruit molecular motors to microtubules, and facilitate microtubule-based transport [39, 40]. Mitochondria are prominent microtubule-based axonal transported organelles, and elevated acetylation of α-tubulin by HDAC6 inhibition can ameliorate mitochondrial transport deficits [15, 36]. In our model of cisplatin-elicited cognitive impairment, HDAC6 inhibition with ACY1215 enhanced α-tubulin acetylation. Concurrently, ACY1215 prevented the cisplatin-induced reduction in mitochondrial accumulation in the neurite and ameliorated cisplatin-induced mitochondrial transport deficits. Interestingly, ACY1215 treatment restored brain mitochondrial dysfunction induced by cisplatin in mice. HDAC6 inhibition has been demonstrated to promote mitochondrial fusion/elongation and increase mitochondrial bioenergetics in cultured neurons [17, 41]. In addition, HDAC6 inhibition suppresses elevated ROS and Ca^{2+} levels and exerts mitochondrial protection via growing acetylation of peroxiredoxin [26]. However, the exact mechanism of how HDAC6 inhibitor ACY1215 enhances mitochondrial bioenergetics and improves mitochondrial function in our model needs further investigation.

Mitochondrial transport has been commonly known as a general index for axonal organelle transport [42]. Active axonal transport of proteins and organelles is essential for neurotransmission, axonal outgrowth, and synapse formation [43]. However, the perturbation of microtubule-based axonal transport may disrupt mitochondrial traffic between neuronal cell bodies and neurites, further give rise to mitochondrial dysfunction, lead to the loss of spines and neurodegeneration. Our results found that synaptic injury was paralleled with impaired axonal transport and mitochondrial dysfunction in cisplatin-treated mice. Notably, ACY1215 mitigated the cisplatin-induced axonal transport defects and mitochondrial dysfunction, and further improved synaptic injury as manifested by the measures of dendritic spines and synaptic density. The amelioration of impaired axonal transport and mitochondrial damage in the CNS appears to be viable strategies to protect synaptic plasticity and delay the cognitive decline [44, 45]. The protective effects of ACY1215 on cognition might benefit from enhancing axonal transport and ameliorating mitochondrial dysfunction.

Few limitations of this study, along with questions for future research, should be noted. First of all, this study was performed in healthy, hormonally, and immunologically intact animals rather than tumor-bearing animals. One recent study revealed that tumor growth might aggravate the development of chemobrain [46]. Whether the protective effects of ACY-1215 on chemobrain in tumor-bearing animals deserves further investigations. Moreover, although the impact of ACY-1215 on body weight was monitored, the other features were undetermined. Lastly, due to acute and short term toxicity test, further investigations should focus on the longitudinal aspects of the possible protective effect of ACY-1215.

Overall, ACY1215 reverses cisplatin-induced cognitive deficit in mice. The protective effect of HDAC6 inhibition is correlated with improved mitochondrial/synaptic dysfunction and enhanced axonal mitochondrial transport via the up-regulation of α-tubulin acetylation. Based on these findings, HDAC6 inhibitor ACY1215 could be a promising candidate for the prevention and treatment of CRCI.

Acknowledgements The present work was supported by National Natural Science Foundation of China (81601225 and U1804174), Henan Provincial Key Research and Development and Promotion Project (192102310081), Science and Technology Innovation Talents in the Universities of Henan Province (20HASTIT044), Science & Technology Innovation teams in Universities of Henan Province (18IRTSTHN026), Outstanding Youth of Science and Technology Innovation in Henan Province (184100510006), Student Research Training Program of Henan University of Science and Technology (2019314).

References

1. de Moor JS, Mariotto AB, Parry C, Alfano CM, Padgett L, Kent EE, Forsythe L, Scoppa S, Hachey M, Rowland JH (2013) Cancer survivors in the United States: prevalence across the survivorship trajectory and implications for care. Cancer Epidemiol Biomark Prev 22:561–570
2. Argyriou AA, Assimakopoulos K, Iconomou G, Giannakopoulou F, Kalofonos HP (2011) Either called "chemobrain" or "chemofog," the long-term chemotherapy-induced cognitive decline in cancer survivors is real. J Pain Symptom Manage 41:126–139
3. Weiss B (2008) Chemobrain: a translational challenge for neurotoxicology. Neurotoxicology 29:891–898
4. Ahles TASaykin AJ (2007) Candidate mechanisms for chemotherapy-induced cognitive changes. Nat Rev Cancer 7:192–201
5. Screnci D, McKeage MJ, Galettis P, Hambley TW, Palmer BD, Baguley BC (2000) Relationships between hydrophobicity, reactivity, accumulation and peripheral nerve toxicity of a series of platinum drugs. Br J Cancer 82:966–972
6. Koppen C, Reifschneider O, Castanheira I, Sperling M, Karst U, Ciarimboli G (2015) Quantitative imaging of platinum based on laser ablation-inductively coupled plasma-mass spectrometry to investigate toxic side effects of cisplatin. Metallomics 7:1595–1603
7. Dzagnidze A, Katsarava Z, Makhalova J, Liedert B, Yoon MS, Kaube H, Limmroth V, Thomale J (2007) Repair capacity for platinum-DNA adducts determines the severity of cisplatin-induced peripheral neuropathy. J Neurosci 27:9451–9457
8. Giurgiovich AJ, Diwan BA, Olivero OA, Anderson LM, Rice JM, Poirier MC (1997) Elevated mitochondrial cisplatin-DNA adduct levels in rat tissues after transplacental cisplatin exposure. Carcinogenesis 18:93–96

9. Olivero OA, Semino C, Kassim A, Lopez-Larraza DM, Poirier MC (1995) Preferential binding of cisplatin to mitochondrial DNA of Chinese hamster ovary cells. Mutat Res 346:221–230
10. Lomeli N, Di K, Czerniawski J, Guzowski JF, Bota DA (2017) Cisplatin-induced mitochondrial dysfunction is associated with impaired cognitive function in rats. Free Radic Biol Med 102:274–286
11. Park HS, Kim CJ, Kwak HB, No MH, Heo JW, Kim TW (2018) Physical exercise prevents cognitive impairment by enhancing hippocampal neuroplasticity and mitochondrial function in doxorubicin-induced chemobrain. Neuropharmacology 133:451–461
12. Chiu GS, Maj MA, Rizvi S, Dantzer R, Vichaya EG, Laumet G, Kavelaars A, Heijnen CJ (2017) Pifithrin-mu prevents cisplatin-induced chemobrain by preserving neuronal mitochondrial function. Cancer Res 77:742–752
13. Hubbert C, Guardiola A, Shao R, Kawaguchi Y, Ito A, Nixon A, Yoshida M, Wang XF, Yao TP (2002) HDAC6 is a microtubule-associated deacetylase. Nature 417:455–458
14. Zhang Y, Li N, Caron C, Matthias G, Hess D, Khochbin S, Matthias P (2003) HDAC-6 interacts with and deacetylates tubulin and microtubules in vivo. EMBO J 22:1168–1179
15. Chen S, Owens GC, Makarenkova H, Edelman DB (2010) HDAC6 regulates mitochondrial transport in hippocampal neurons. PLoS ONE 5:e10848
16. Zhang L, Liu C, Wu J, Tao JJ, Sui XL, Yao ZG, Xu YF, Huang L, Zhu H, Sheng SL, Qin C (2014) Tubastatin A/ACY-1215 improves cognition in Alzheimer's disease transgenic mice. J Alzheimers Dis 41:1193–1205
17. Krukowski K, Ma J, Golonzhka O, Laumet GO, Gutti T, van Duzer JH, Mazitschek R, Jarpe MB, Heijnen CJ, Kavelaars A (2017) HDAC6 inhibition effectively reverses chemotherapy-induced peripheral neuropathy. Pain 158:1126–1137
18. Zhou W, Kavelaars A, Heijnen CJ (2016) Metformin prevents cisplatin-induced cognitive impairment and brain damage in mice. PLoS ONE 11:e0151890
19. Santo L, Hideshima T, Kung AL, Tseng JC, Tamang D, Yang M, Jarpe M, van Duzer JH, Mazitschek R, Ogier WC, Cirstea D, Rodig S, Eda H, Scullen T, Canavese M, Bradner J, Anderson KC, Jones SS, Raje N (2012) Preclinical activity, pharmacodynamic, and pharmacokinetic properties of a selective HDAC6 inhibitor, ACY-1215, in combination with bortezomib in multiple myeloma. Blood 119:2579–2589
20. Park H, Kang S, Nam E, Suh YH, Chang KA (2019) The protective effects of PSM-04 against beta amyloid-induced neurotoxicity in primary cortical neurons and an animal model of Alzheimer's disease. Front Pharmacol 10:2
21. Dragicevic N, Mamcarz M, Zhu Y, Buzzeo R, Tan J, Arendash GW, Bradshaw PC (2010) Mitochondrial amyloid-beta levels are associated with the extent of mitochondrial dysfunction in different brain regions and the degree of cognitive impairment in Alzheimer's transgenic mice. J Alzheimers Dis 20(Suppl 2):S535–S550
22. Wang D, Liu X, Liu Y, Shen G, Zhu X, Li S (2017) Treatment effects of Cardiotrophin-1 (CT-1) on streptozotocin-induced memory deficits in mice. Exp Gerontol 92:42–45
23. Wang D, Liu X, Liu Y, Li S, Wang C (2017) The effects of cardiotrophin-1 on early synaptic mitochondrial dysfunction and synaptic pathology in APPswe/PS1dE9 mice. J Alzheimers Dis 59:1255–1267
24. Li SQ, Wang DM, Shu YJ, Wan XD, Xu ZS, Li EZ (2013) Proper heat shock pretreatment reduces acute liver injury induced by carbon tetrachloride and accelerates liver repair in mice. J Toxicol Pathol 26:365–373
25. Liu Y, Zhang Z, Qin Y, Wu H, Lv Q, Chen X, Deng W (2013) A new method for Schwann-like cell differentiation of adipose derived stem cells. Neurosci Lett 551:79–83
26. Choi H, Kim HJ, Kim J, Kim S, Yang J, Lee W, Park Y, Hyeon SJ, Lee DS, Ryu H, Chung J, Mook-Jung I (2017) Increased acetylation of Peroxiredoxin1 by HDAC6 inhibition leads to recovery of Abeta-induced impaired axonal transport. Mol Neurodegener 12:23
27. Govindarajan N, Rao P, Burkhardt S, Sananbenesi F, Schluter OM, Bradke F, Lu J, Fischer A (2013) Reducing HDAC6 ameliorates cognitive deficits in a mouse model for Alzheimer's disease. EMBO Mol Med 5:52–63
28. Pareyson D, Piscosquito G, Moroni I, Salsano E, Zeviani M (2013) Peripheral neuropathy in mitochondrial disorders. Lancet Neurol 12:1011–1024
29. Bindu PS, Govindaraju C, Sonam K, Nagappa M, Chiplunkar S, Kumar R, Gayathri N, Bharath MM, Arvinda HR, Sinha S, Khan NA, Govindaraj P, Nunia V, Paramasivam A, Thangaraj K, Taly AB (2016) Peripheral neuropathy in genetically characterized patients with mitochondrial disorders: A study from south India. Mitochondrion 27:1–5
30. Olivero OA, Chang PK, Lopez-Larraza DM, Semino-Mora MC, Poirier MC (1997) Preferential formation and decreased removal of cisplatin-DNA adducts in Chinese hamster ovary cell mitochondrial DNA as compared to nuclear DNA. Mutat Res 391:79–86
31. Podratz JL, Knight AM, Ta LE, Staff NP, Gass JM, Genelin K, Schlattau A, Lathroum L, Windebank AJ (2011) Cisplatin induced mitochondrial DNA damage in dorsal root ganglion neurons. Neurobiol Dis 41:661–668
32. Yang Z, Schumaker LM, Egorin MJ, Zuhowski EG, Guo Z, Cullen KJ (2006) Cisplatin preferentially binds mitochondrial DNA and voltage-dependent anion channel protein in the mitochondrial membrane of head and neck squamous cell carcinoma: possible role in apoptosis. Clin Cancer Res 12:5817–5825
33. Martins NM, Santos NA, Curti C, Bianchi ML, Santos AC (2008) Cisplatin induces mitochondrial oxidative stress with resultant energetic metabolism impairment, membrane rigidification and apoptosis in rat liver. J Appl Toxicol 28:337–344
34. Zsengeller ZK, Ellezian L, Brown D, Horvath B, Mukhopadhyay P, Kalyanaraman B, Parikh SM, Karumanchi SA, Stillman IE, Pacher P (2012) Cisplatin nephrotoxicity involves mitochondrial injury with impaired tubular mitochondrial enzyme activity. J Histochem Cytochem 60:521–529
35. Chiou CT, Wang KC, Yang YC, Huang CL, Yang SH, Kuo YH, Huang NK (2018) Liu Jun Zi Tang-A: potential, multi-herbal complementary therapy for chemotherapy-induced neurotoxicity. Int J Mol Sci 19:1258
36. d'Ydewalle C, Krishnan J, Chiheb DM, Van Damme P, Irobi J, Kozikowski AP, Vanden Berghe P, Timmerman V, Robberecht W, Van Den Bosch L (2011) HDAC6 inhibitors reverse axonal loss in a mouse model of mutant HSPB1-induced Charcot-Marie-Tooth disease. Nat Med 17:968–974
37. Dompierre JP, Godin JD, Charrin BC, Cordelieres FP, King SJ, Humbert S, Saudou F (2007) Histone deacetylase 6 inhibition compensates for the transport deficit in Huntington's disease by increasing tubulin acetylation. J Neurosci 27:3571–3583
38. Godena VK, Brookes-Hocking N, Moller A, Shaw G, Oswald M, Sancho RM, Miller CC, Whitworth AJ, De Vos KJ (2014) Increasing microtubule acetylation rescues axonal transport and locomotor deficits caused by LRRK2 Roc-COR domain mutations. Nat Commun 5:5245
39. Bulinski JC (2007) Microtubule modification: acetylation speeds anterograde traffic flow. Curr Biol 17:R18–R20
40. Reed NA, Cai D, Blasius TL, Jih GT, Meyhofer E, Gaertig J, Verhey KJ (2006) Microtubule acetylation promotes kinesin-1 binding and transport. Curr Biol 16:2166–2172
41. Guedes-Dias P, de Proenca J, Soares TR, Leitao-Rocha A, Pinho BR, Duchen MR, Oliveira JM (2015) HDAC6 inhibition induces mitochondrial fusion, autophagic flux and reduces diffuse

mutant huntingtin in striatal neurons. Biochim Biophys Acta 1852:2484–2493
42. Hollenbeck PJSaxton WM (2005) The axonal transport of mitochondria. J Cell Sci 118:5411–5419
43. Liu XA, Rizzo V, Puthanveettil SV (2012) Pathologies of axonal transport in neurodegenerative diseases. Transl Neurosci 3:355–372
44. Lin MTBeal MF (2006) Mitochondrial dysfunction and oxidative stress in neurodegenerative diseases. Nature 443:787–795
45. Riemer JKins S (2013) Axonal transport and mitochondrial dysfunction in Alzheimer's disease. Neurodegener Dis 12:111–124
46. Winocur G, Berman H, Nguyen M, Binns MA, Henkelman M, van Eede M, Piquette-Miller M, Sekeres MJ, Wojtowicz JM, Yu J, Zhang H, Tannock IF (2018) Neurobiological mechanisms of chemotherapy-induced cognitive impairment in a transgenic model of breast. Cancer Neurosci 369:51–65

Affiliations

Dongmei Wang[1] · Bei Wang[1] · Yumei Liu[2] · Xiaohui Dong[1] · Yanwei Su[1] · Sanqiang Li[1]

✉ Dongmei Wang
wdmzgadyx@hotmail.com

✉ Sanqiang Li
sanqiangli2001@163.com

[1] Medical College, Henan University of Science and Technology, Luoyang 471023, People's Republic of China

[2] College of Animal Science and Technology, Henan University of Science and Technology, Luoyang, People's Republic of China